Supplementary Information

Novel structurally-stable Na-rich Na$_4$V$_2$O$_7$ cathode material with high reversible capacity by utilization of anion redox activity

Experimental section

Synthesis

Na$_4$V$_2$O$_7$ was synthesized by a facile solid-state reaction method. V$_2$O$_5$ (Sigma Aldrich, 99%) and NaHCO$_3$ (Alfa Aesar, 99%) were mixed by ball milling (Fritsch Pulverisette 7) with a speed of 300 rpm for 4 hr in ethanol. The mixed precursors were pressed into pellets after evaporating the ethanol, followed by heating in flowing air at 400 °C for 12 hr in an alumina crucible with a ramp rate of 2 °C min^{-1}. The sample was directly transferred to an argon-filled glovebox before cooling. The as-prepared Na$_4$V$_2$O$_7$ is white in color. Since the material has low electronic conductivity due to presence of V^{5+} (d0 configuration), the obtained Na$_4$V$_2$O$_7$ was further ball-milled with acetylene black (AB) with a weight ratio of 60:30 at 400 rpm for 3 hr in Ar to increase its electrical conductivity.

Electrochemistry

To evaluate the performance of Na$_4$V$_2$O$_7$ as a Na-ion battery cathode material, composite electrodes were fabricated by casting a mixed slurry of ball-milled powder (Na$_4$V$_2$O$_7$ with AB) and polyvinylidene fluoride (PVdF) binder (90:10 by weight) in 1-methyl-2-pyrrolidone (NMP) onto a carbon-coated aluminum current collector (MTIXTL). For comparison, electrodes were also prepared with the as-prepared Na$_4$V$_2$O$_7$ mixed with AB with a weight ratio of 60:30 with a mortar and pestle for 20 mins. All procedures were conducted in a glovebox without exposure in air due to the high hygroscopicity of Na$_4$V$_2$O$_7$. Electrodes with a diameter of 16 mm were cut and then pressed by a calender after drying. The mass loading of active material on each electrode is about 2.2-2.7 mg, corresponding to an average loading of 1.2 mg cm^{-2}. Coin cells (2032-type) were assembled in an argon-filled glovebox using 2 M NaPF$_6$ in propylene carbonate (PC) as the electrolyte, a glass fiber filter as separator and sodium metal as counter electrode. Galvanostatic cycling was carried out with a battery tester (Neware) at 25 °C with a typical current rate of 10 mA g^{-1} between 1.2 and 4.7 V (or 4.4 V) vs. Na/Na$^+$. For the preparation of ex-situ samples, electrodes were cycled to different charge/discharge states and then recovered and washed with anhydrous DMC three times in the glovebox and dried in the antechamber under vacuum.

X-ray Photoelectron Spectroscopy (XPS)

XPS was carried out on an Escalab 250 Energy Spectrometer (Thermal Scientific Corporation, USA) using monochromatic Al K$_\alpha$ X-ray source at 1486.6 eV. The etching rate of Ar$^+$ beam is confirmed to be 9 nm min^{-1} based on the Ta$_2$O$_5$ standard sample and the etching time was set to 1 min for our cycled electrodes. The base pressure of the system was 2×10^{-10} mbar, and the spectrometer was calibrated using C1s at 284.4 eV. Samples were transported from the glovebox to the instrument using a dedicated transfer chamber to avoid contact with air.

Powder X-ray Diffraction

Phase identification of the $Na_4V_2O_7$ samples was conducted using laboratory powder X-ray diffraction using a Cu Kα radiation source (λ=1.5418 Å) with a PANalytical X'Pert3 X-ray Diffractometer. For detailed structural analysis of the as-synthesized materials, synchrotron powder X-ray diffraction (XRD) data were collected at the Powder Diffraction Beamline at the Australian Synchrotron, ANSTO, with an incident wavelength of 0.6875(6) Å for powder test and 0.7273(1) Å for electrode test determined using a LaB_6 standard reference material. XRD data were collected on a coin cell with transmission geometry every 3.4 mins (with detector position movement). The crystal structure was refined by the Rietveld method using the GSAS-II software.[1] Coin cells with 3 mm diameter Kapton-covered windows in the casings and 5 mm diameter holes in the stainless steel spacers were used for the construction of the coin cells for the *in-situ* XRD measurements.

X-ray Absorption Spectra (XAS)

Synchrotron XAS measurements were conducted at the V K-edge at the XAS beamline at the Australian Synchrotron in Melbourne. Acquisition using a Bruker detector was carried out in fluorescence yield mode with about 100 nm probe depth. The ex-situ cathodes were transferred from an Ar-filled glovebox to the analysis chamber without exposure in air. The data reduction follows standard methods using the DEMETER software package.[2]

Supplementary Figures and Tables
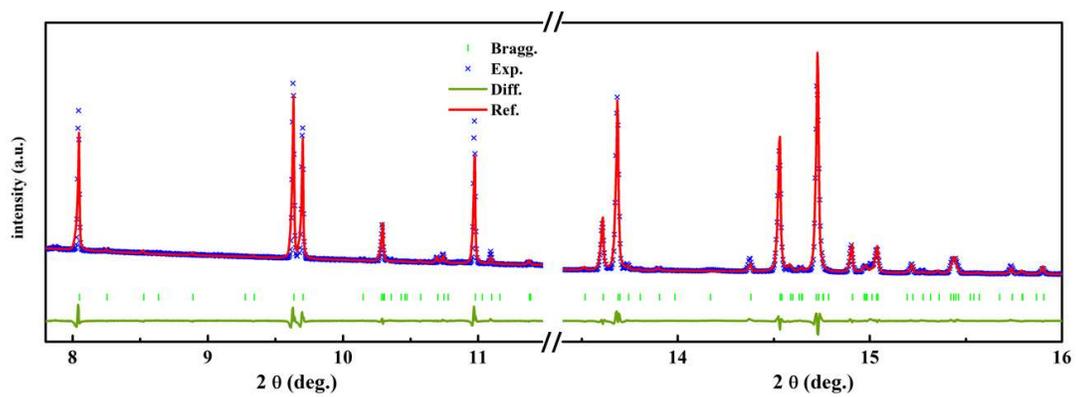
Fig. S1. Rietveld-refined fit of $Na_4V_2O_7$ based on synchrotron XRD data with specific 2θ range for clarification ($\lambda = 0.6875(6)$Å).
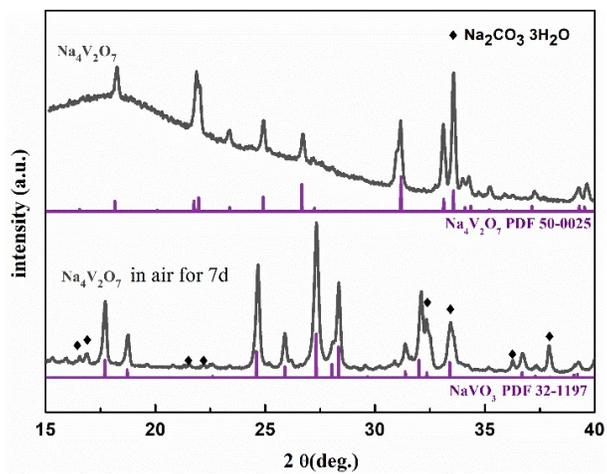
Fig. S2. XRD pattern of as-prepared $Na_4V_2O_7$ and that after exposure in air for 7 days ($\lambda = 1.5418$ Å).
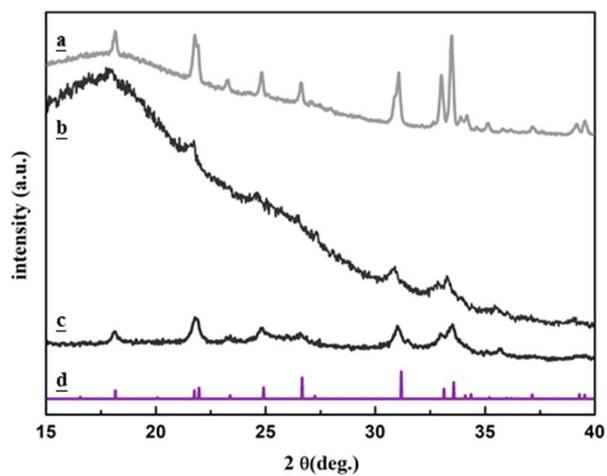
Fig. S3. XRD patterns of (a) $Na_4V_2O_7$ tested with Kapton tape, (b) ball-milled $Na_4V_2O_7$ tested with Kapton tape, (c) ball-milled $Na_4V_2O_7$ tested in air for clarification and (d) $Na_4V_2O_7$ PDF 50-0025 ($\lambda = 1.5418$ Å).
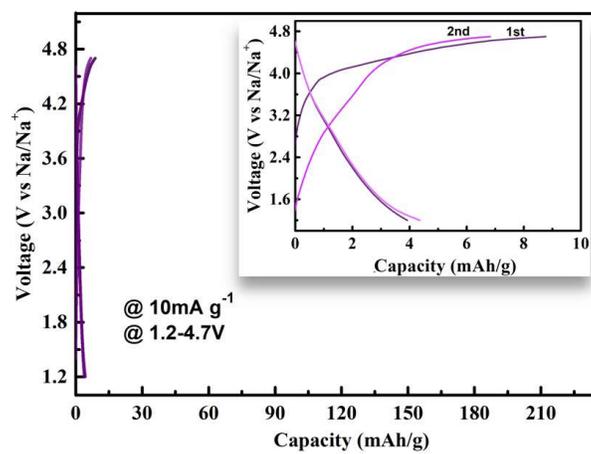
Fig. S4. Charge-discharge curves of $Na_4V_2O_7$ at a current rate of 10 mA g^{-1} in the range of 1.2 - 4.7 V without ball milling with AB.
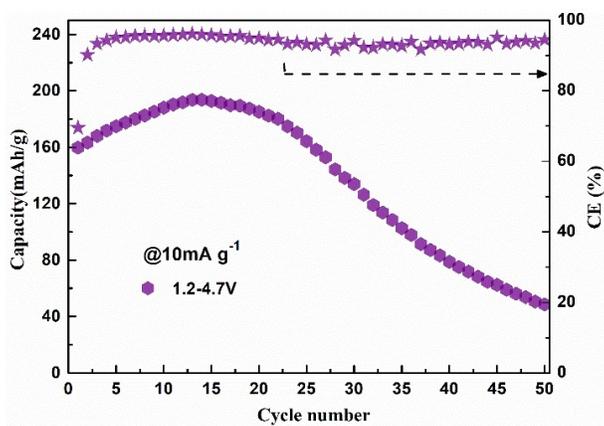
Fig. S5. Cycle performance and Coulombic efficiency of $Na_4V_2O_7$ in the range of 1.2 - 4.7 V at a current rate of 10 mA g^{-1}.
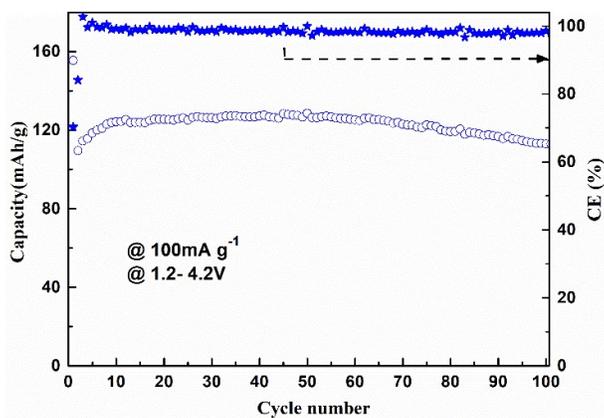
Fig. S6. Cycle performance and Coulombic efficiency of $Na_4V_2O_7$ in the range of 1.2 - 4.2 V at 100 mA g^{-1} after activation to 4.7 V during first charge.
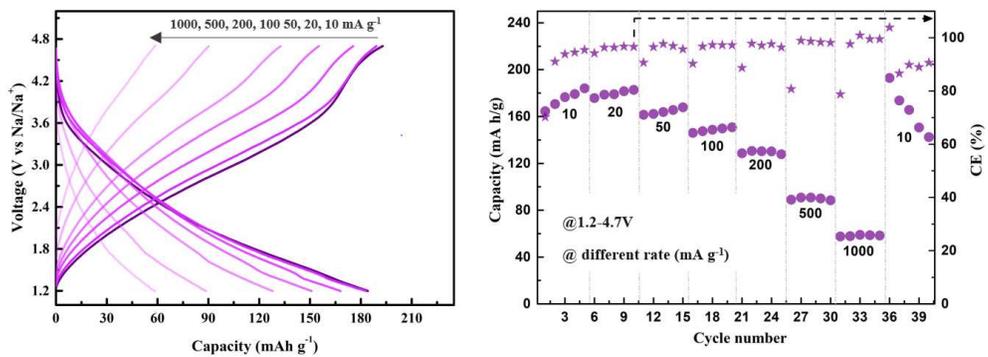
Fig. S7. Rate performance of $Na_4V_2O_7$ in the range of 1.2 - 4.7 V at different current rates.
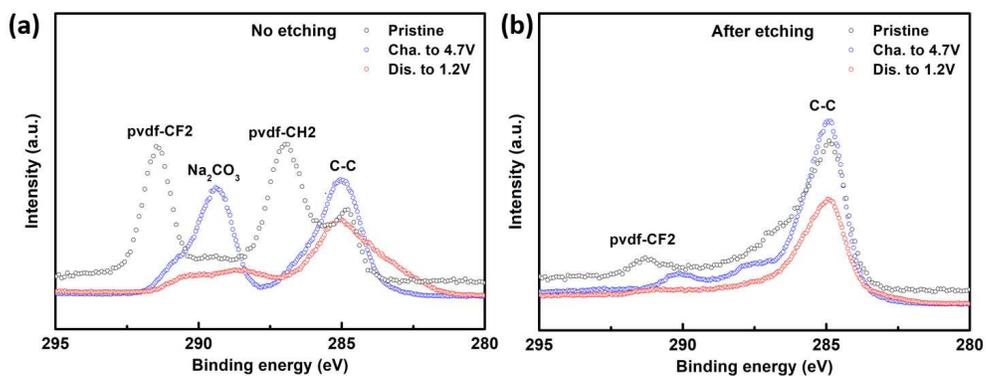
Fig. S8 XPS core spectra of C 1s at different states: pristine, charged to 4.7 V and discharged to 1.2 V (a) without Ar ion etching and (b) with Ar ion etching to reduce the surface deposits.

In the carbon spectra, there are apparent CF_2 and CH_2 signals from the PVdF binder in the pristine electrode. After charge and discharge, the signals from PVdF mostly disappeared indicating there are complex deposits on the surface of electrode (i.e. solid electrolyte interface, Na_2CO_3). After Ar^+ etching, the peak corresponding to C-C signal dominates after most surface deposits have been disposed of. (There is only a small signal of PVdF in pristine electrode after Ar^+ etching since PVdF can be destroyed by the Ar ion beam)
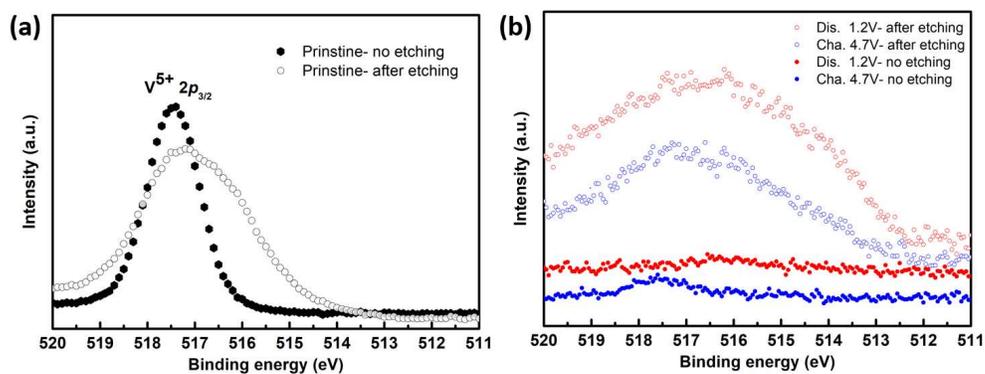
Fig. S9 XPS core spectra of V $2p_{3/2}$ at different states: (a) pristine and (b) charged to 4.7 V and discharged to 1.2 V with or without Ar ion etching.

In the vanadium spectra (Fig. S9), the pristine material shows a main XPS peak corresponding V^{5+}. After Ar^+ etching, a new peak emerges at a lower binding energy, indicating that V^{5+} has been reduced. So, the V XPS is susceptible to how the experiments are done.
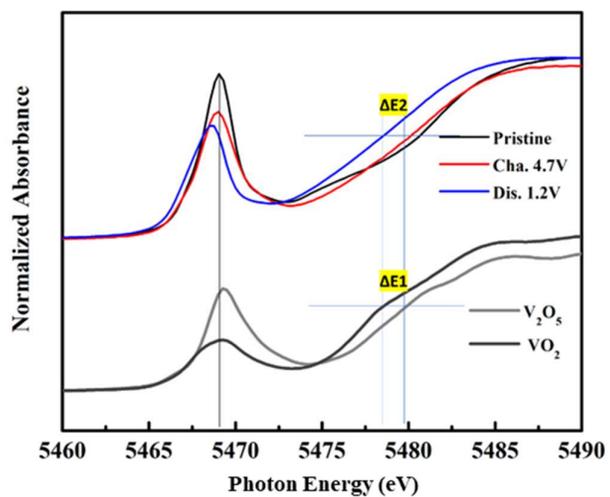
Fig. S10. Normalized V K-edge XANES spectra collected from commercial VO_2 and V_2O_5, in comparison with the $Na_4V_2O_7$ electrodes (top) at different charge-discharge states.
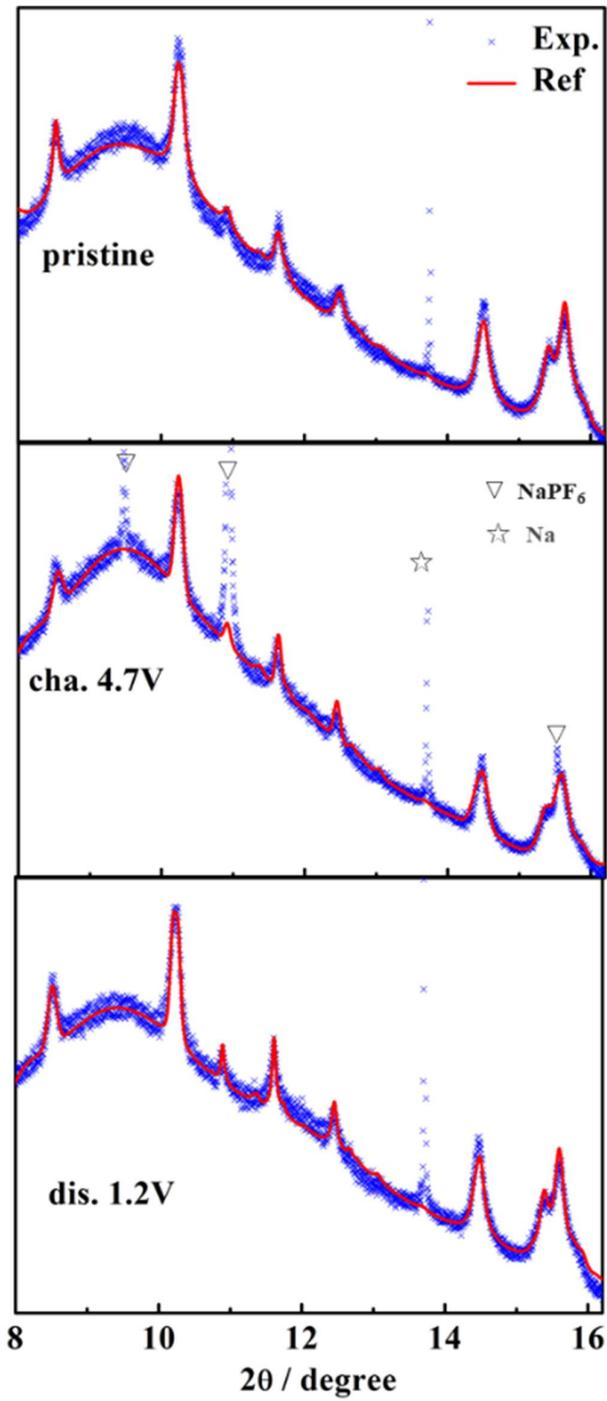
Fig. S11. Refinement of specific XRD of pristine electrode, one charged to 4.7 V, and one discharged to 1.2 V ($\lambda = 0.7273(1)$ Å).
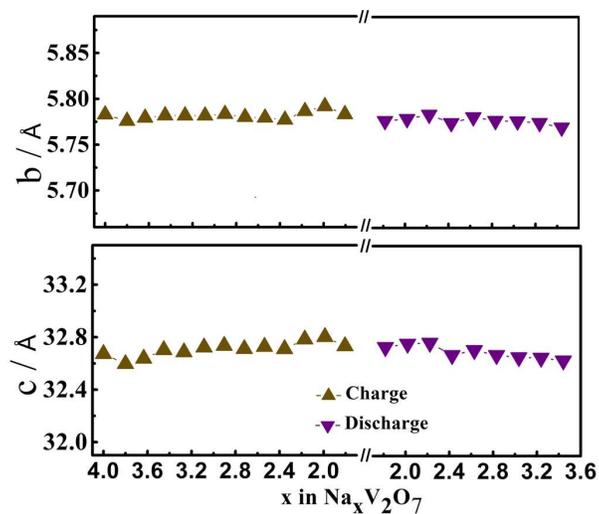
Fig. S12. Evolution of the lattice parameters b and c during Na deintercalation and intercalation at different sodium content (x) in $Na_xV_2O_7$.

Reference:
1. B. H. Toby and R. B. Von Dreele, *Journal of Applied Crystallography*, 2013, **46**, 544-549.
2. B. Ravel and M. Newville, *Journal of Synchrotron Radiation*, 2005, **12**, 537-541.